

3. Wen PY, Alyea EP, Simon D, Herbst RS, Soiffer RJ, Antin JH. Guillain-Barre syndrome following allogeneic bone marrow transplantation. *Neurology*. 1997;49:1711–4.
4. Ponticelli C, Campise MR. Neurological complications in kidney transplant recipients. *J Nephrol*. 2005;18:521–8.
5. Dionne A, Nicolle MW, Hahn AF. Clinical and electrophysiological parameters distinguishing acute-onset chronic inflammatory demyelinating polyneuropathy from acute inflammatory demyelinating polyneuropathy. *Muscle Nerve*. 2010;41:202–7.
6. Labate A, Morelli M, Palamara G, Pirritano D, Quattrone A. Tacrolimus-induced polyneuropathy after heart transplantation. *Clin Neuropharmacol*. 2010;33:161–2.

Servicio de Nefrología, Hospital del Bierzo, Ponferrada, España

* Autor para correspondencia.

Correo electrónico: Igor9843@gmail.com

(I. Romaniouk Jakovler).

0211-6995/© 2017 Sociedad Española de Nefrología. Publicado por Elsevier España, S.L.U. Este es un artículo Open Access bajo la licencia CC BY-NC-ND (<http://creativecommons.org/licenses/by-nc-nd/4.0/>).

<https://doi.org/10.1016/j.nefro.2017.11.005>

Igor Romaniouk Jakovler*, Carmen Perez Nieto, Marco Romero Antonio, Fernando Simal Blanco y Ricardo Mouzo Javier

Triple functioning renal allograft after repeated liver–kidney transplantation due to liver failure

Funcionamiento de un triple trasplante renal alogénico tras repetir un trasplante de hígado-riñón por fallo hepático

A 56-year-old woman who underwent 10 years earlier simultaneous liver–kidney transplantation due to polycystic

disease (Fig. 1A) showed progressive transaminase elevation secondary to hepatotoxicity due to venlafaxine. The patient

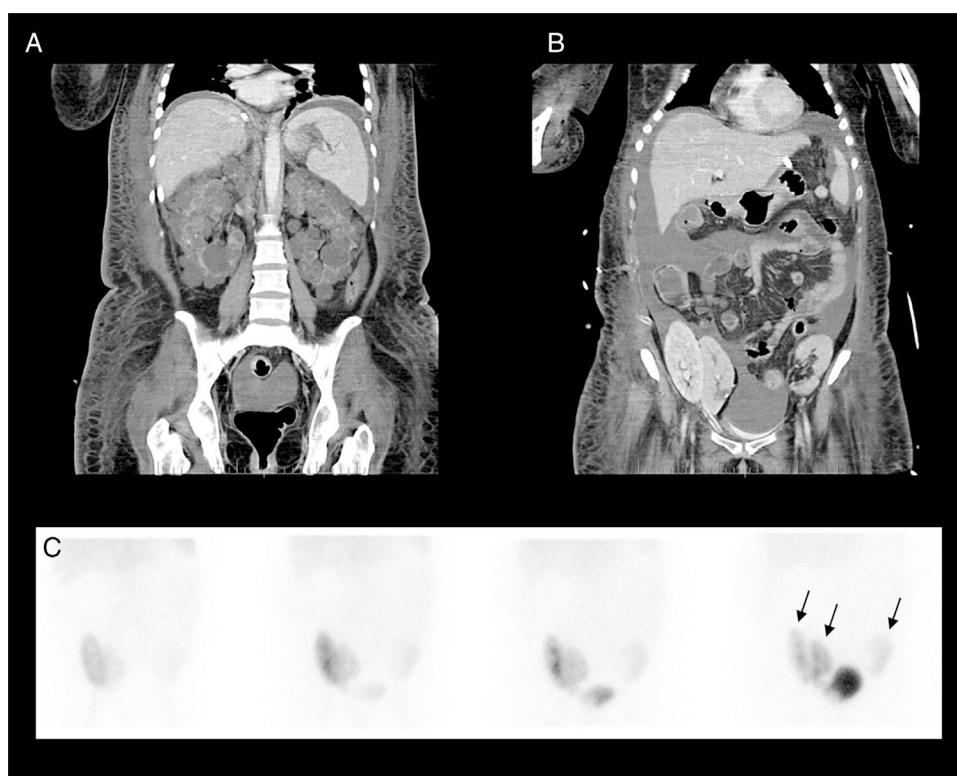


Fig. 1 – Baseline CT coronal views show polycystic kidneys before the first liver–kidney transplantation (A). Follow-up CT locates the three transplanted kidneys in both sides of the pelvis (B). A renogram study using ^{99m}Tc-MAG₃ was performed identifying different degrees of radiotracer uptake in all three transplanted kidneys (C).

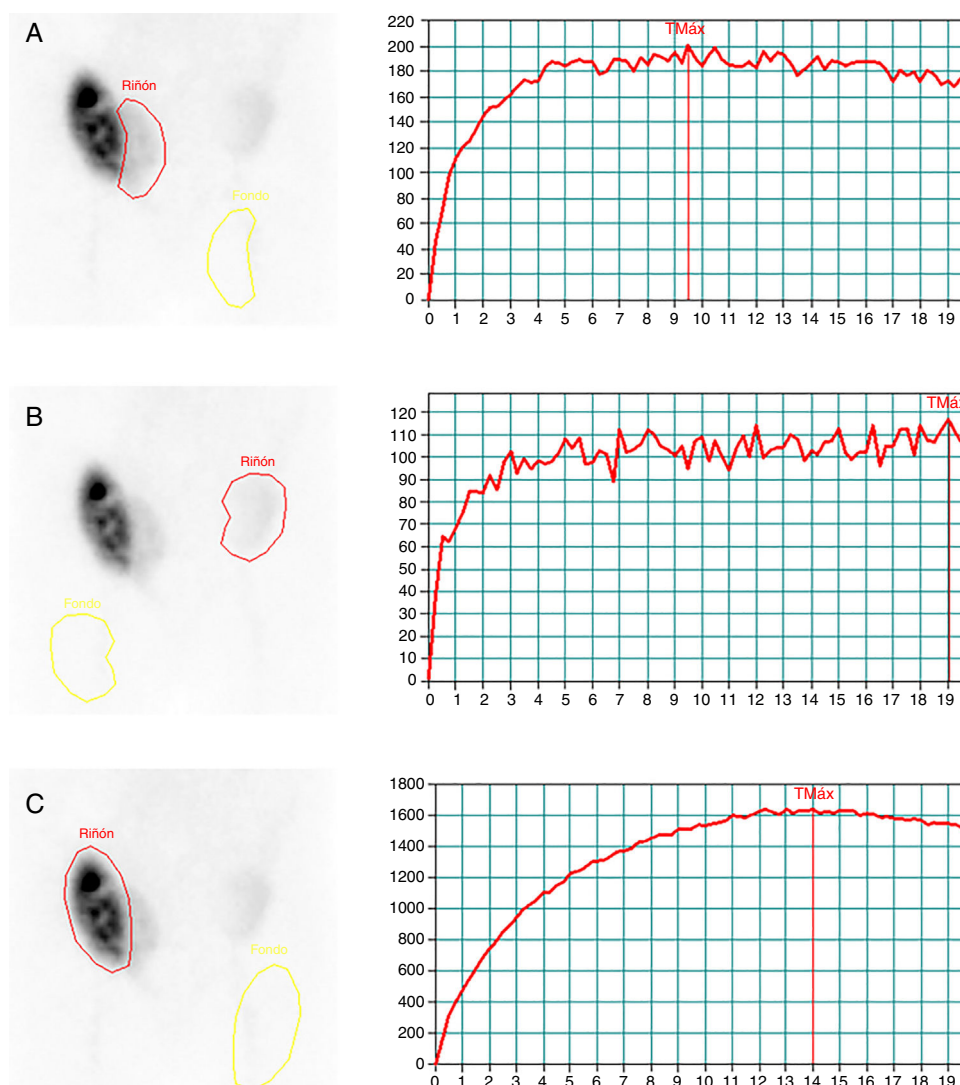


Fig. 2 – $^{99m}\text{Tc-MAG}_3$ renogram curves were generated after drawing whole-kidney and background regions of interest for each renal transplant. The results obtained were expressed as the maximum count ratios: 200 cps (A), 117 cps (B) and 1640 cps (C), respectively. The relative differential function showed the following distribution of 16% for the right medial graft (A), 9% for the left graft (B) and 75% for the right lateral graft (C).

was diagnosed of liver rejection and retransplant was required. However, the patient also presented progressive renal failure worsened by liver failure (Cr 4.5 mg/dL), so a second simultaneous liver-kidney transplant was performed to prevent subsequent dialysis. Fifteen days later showed a prominent liver graft dysfunction and again was candidate for a new liver transplant. At this point, the second kidney graft was dysfunctional and considered as acute tubular necrosis by ultrasound. A third simultaneous liver-kidney transplant was considered and finally performed without remarkable incidences (Fig. 1B). Renogram has been widely used in the follow-up of renal transplant function and has proved reliable to define the integrity of the kidney. The current case shows functional recovery of all three transplanted kidneys demonstrated by the renogram images (Fig. 1C) and the correspondent generated curves for each renal transplant (Fig. 2). To our knowledge, this is a rare case not previously reported

which raises the question about the need of systematic kidney transplantation when a liver transplant is required.^{1,2}

BIBLIOGRAFÍA

1. Aparici CM, Bains SN, Carlson D, Qian J, Liou D, Wojciechowki D, et al. Recovery of native renal function in patients with hepatorenal syndrome following combined liver and kidney transplant with mercaptoacetyltriglycine-3 renogram: developing a methodology. *World J Nucl Med.* 2016;15:44-9.
2. Palmer MR, Donohoe KJ, Francis JMA, Mandelbrot D. Evaluation of relative renal function for patients who had undergone simultaneous liver-kidney transplants using Tc-99m-MAG3 scintigraphy with attenuation correction from anatomical images and SPECT/CT. *Nucl Med Commun.* 2011;32: 738-44.

Andrés Tapias^a, Nuria Sánchez^a, José V. Torregrosa^b,
David Fuster^{a,*}, Pilar Perlaza^a, Francisco Lomeña^a

^a Nuclear Medicine Department, Hospital Clinic, Barcelona, Spain

^b Nephrology and Renal Transplant Department, Hospital Clinic,
Barcelona, Spain

* Corresponding author.

E-mail address: dfuster@clinic.ub.es (D. Fuster).

0211-6995/© 2018 Sociedad Española de Nefrología. Published
by Elsevier España, S.L.U. This is an open access article
under the CC BY-NC-ND license (<http://creativecommons.org/licenses/by-nc-nd/4.0/>).

<https://doi.org/10.1016/j.nefro.2017.11.014>

IgA-dominant infection-related glomerulonephritis

Glomerulonefritis relacionada con la infección por IgA-Dominante

Dear Editor:

Acute post-infectious glomerulonephritis is an immune complex-mediated glomerulonephritis that classically occurs in children following streptococcal upper respiratory or skin infections. However, cases of IgA-dominant infection-related glomerulonephritis (IgA-IRGN), a diffuse endocapillary proliferative glomerulonephritis associated with intense IgA deposits following staphylococcus infection, have been increasingly reported in recent literature. In contrast to typical acute post-infectious glomerulonephritis, the causative infection is ongoing at the time of diagnosis.¹ It often occurs in diabetic elderly patients and presents with acute kidney injury and heavy proteinuria. The prognosis is unfavourable. Here, we report an elderly-male patient with IgA-IRGN who demonstrated vasculitic skin rash.

An 80-year-old Japanese man with stage G3a chronic kidney disease due to diabetes mellitus was admitted to the general medicine service for management of right haemopneumothorax after a motor vehicle accident and subsequent empyema caused by methicillin-sensitive *Staphylococcus aureus* treated with four weeks of intravenous cefazolin and drainage. The patient was seen in nephrology consultation for a rise in serum creatinine level from 1.4 mg/dl upon admission to 5.3 mg/dl (estimated glomerular filtration rate of 9 ml/min/1.73 m²) and purpuric lesions on the bilateral lower extremities. At the general medicine service, oral glucocorticoid was initiated for a presumed diagnosis of IgA vasculitis (Henoch-Schönlein purpura). However, the kidney function continued to worsen, and oliguria ensued despite infusion of lactated ringer's solution. Upon physical examination, he was not in distress. The blood pressure was 110/78 mmHg. There were trace pretibial oedema and purpuric lesions on the bilateral legs. Urinalysis showed >100 red blood cells per high-power field (70% dysmorphic) and 5.2 g/24 h of proteinuria. Immunological analysis showed that increased immunoglobulins (IgG 1427 mg/dl; IgA 1373 mg/dl; IgM 48 mg/dl) and decreased complement levels (C3 77 mg/dl; C4 30 mg/dl; CH50 44 IU/ml). Antinuclear

antibodies, antimyeloperoxidase antibodies, antiproteinase 3 antibodies, and a glomerular basement membrane antibody were negative. Renal biopsy showed 10 glomeruli, 4 of them sclerosed and 2 with endocapillary proliferation (Fig. 1). There was a mild interstitial infiltrate of polymorphonuclear cells, and the arteries had no significant lesions. Immunofluorescence microscopy showed diffuse depositions of IgA (Fig. 2) and C3. Electron microscopy could not be performed because of insufficient specimens. Based on clinical features and pathologic findings, IgA-IRGN was diagnosed. Intravenous cefazolin was administered for another four weeks, and oral glucocorticoid was tapered and stopped gradually without relapse of infection. However, the patient progressed to end-stage kidney disease even after 20 mg of olmesartan was initiated.

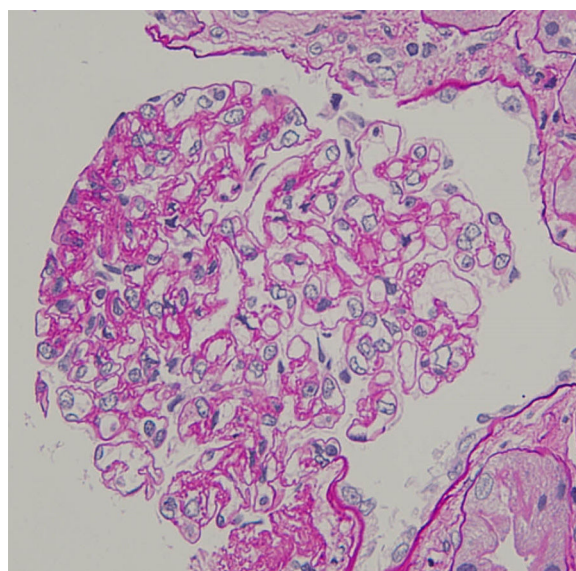


Fig. 1 – Renal biopsy (haematoxylin and eosin, ×400), showing endocapillary hypercellularity with immune cell infiltration (arrow head).